Optical Coherence Tomography

The Intraoperative Assessment of Lymph Nodes in Breast Cancer

BY FREDDY T. NGUYEN, ADAM M. ZYSK, ERIC J. CHANEY, STEVEN G. ADIE, JAN G. KOTYNEK, URETZ J. OLIPHANT, FRANK J. BELLAFIORE, KENDRITH M. ROWLAND, PATRICIA A. JOHNSON, AND STEPHEN A. BOPPART

During breast-conserving surgeries, axillary lymph nodes draining from the primary tumor site are removed for disease staging. Although a high number of lymph nodes are often resected during sentinel and lymph-node dissections, only a relatively small percentage of nodes are found to be metastatic, a fact that must be weighed against potential complications such as lymphedema. Without a real-time in vivo or in situ intraoperative imaging tool to provide a microscopic assessment of the nodes, postoperative paraffin section histopathological analysis currently remains the gold standard in assessing the status of lymph nodes. Optical coherence tomography (OCT), a high-resolution real-time microscopic optical-imaging technique previously used to image breast cancer tumor margins intraoperatively in humans and lymph-node microarchitecture in a rat animal model, is being presented for the intraoperative ex vivo imaging and assessment of axillary lymph nodes. OCT provides real-time microscopic images up to 2 mm beneath the tissue surface in axillary lymph nodes. Normal (13), reactive (1), and metastatic (3) lymph nodes from 17 human patients with breast cancer were imaged intraoperatively with OCT. These preliminary clinical studies have identified scattering changes in the cortex, relative to the capsule, which can be used to differentiate normal from reactive and metastatic nodes. These optical scattering changes are correlated with inflammatory and immunological changes observed in the follicles and germinal centers. These results suggest that intraoperative OCT has the potential to assess the real-time node status in situ, without having to physically resect and histologically process specimens to visualize microscopic features.

Breast Cancer

Breast cancer continues to affect a significant proportion of women, as 192,370 new cases of invasive breast cancer and 62,280 cases of ductal carcinoma in situ (DCIS) are expected in the United States during 2009, making it the most widely diagnosed cancer (26% of new cases) in women [1]. The number of deaths attributed to breast cancer (40,610 expected in 2009—second only to lung cancer) has started to decrease over the last few years, largely attributed to the effectiveness of breast-cancer screening [1]. These developments have led to the increased detection of breast-cancer lesions at earlier stages, resulting in smaller breast lesions and a decreased likelihood of lymph-node involvement and cancer metastasis. The management and treatment of breast cancer has continued to improve, as evidenced by the gradual increases in the five-year survival rates for all stages of breast cancer [2]. Currently, patients electing to undergo lumpectomies or mastectomies will typically have a sentinel lymph-node dissection (SLND), which may be accompanied by the removal of additional axillary lymph nodes via axillary lymph-node dissection (ALND) to help stage disease progression [2]. Staging is based on the size of the primary tumor, the involvement of lymph nodes, and the metastatic spread to secondary sites.

Digital Object Identifier 10.1109/MEMB.2009.935722

Mapping of Lymph Nodes

Lymph-node mapping is currently performed by injecting a radioactive tracer (technetium-99) and/or a dye (isosulfan blue) preoperatively near the site of the primary tumor. The tracer and/or dye is allowed to circulate for several hours, after which the sentinel node(s) are located and resected during lumpectomy or mastectomy [3]. Other lymphatic mapping methods include standard X-ray and computed tomography (CT) in conjunction with contrast agents, or fluorescence techniques using near-infrared (NIR) quantum dots [4], [5] or indocyanine green (ICG) dye [6], which provide better localization of the lymph node. Lymph nodes are typically only removed to stage the disease progression via histopathological analysis. A positive sentinel node status will prompt surgeons to consider patients for axillary lymph-node dissections, further node sampling via biopsies, or whole-body imaging to determine the extent of the metastatic spread of cancer.

Current and Experimental Nodal Assessment Techniques

The current standard of care for lymph-node assessment is postoperative paraffin section histopathological analysis. No real-time intraoperative microscopic technique is being currently widely used for the assessment of lymph nodes. The use of frozen-section histopathology of lymph nodes is also an accepted nodal assessment method, but often takes 20–30 min to perform, lengthening the time that the patient is under

Staging is based on the size of the primary tumor, the involvement of lymph nodes, and the metastatic spread to secondary sites.

general anesthesia [7], [8]. Several other intraoperative techniques are currently under investigation, including touch imprint cytology [9], [10], molecular marker assays [11], frozen-section analysis [7], [8], and Fourier transform infrared microspectroscopy [12]. All these techniques require the physical sectioning of the lymph node, leading to the physical destruction of the nodal structural integrity and cellular architecture to perform the molecular assay, staining, or probing protocols. The use of wide-field NIR fluorescence imaging has also been developed to better visualize the dynamics of the lymphatic system [13], [14].

Clinical Importance of Lymph-Node Assessment

Lymph nodes serve as the primary site for filtering, sequestering, and degrading foreign particles that travel through the lymphatic system. They are typically classified as normal, reactive, or metastatic. Both a reactive node and a metastatic node are relatively enlarged in size as lymphocytes and macrophages are recruited to the node in response to the presence of foreign particles or abnormal cells. However, in a metastatic node, there is an increased presence and involvement of cancer cells in addition to the inflammatory response. When the lymphatic system becomes impaired because of the disruption of the lymphatic network, lymphatic obstruction develops, leading to the accumulation of lymph fluid or lymphedema. Currently, nearly 20% of the patients who undergo ALND suffer from these cases of edema [15], [16]. In addition, a recent study reported that the presence of micrometastases in the axillary lymph nodes contributed to a decrease in the five-year survival rates for women with early breast cancer [17].

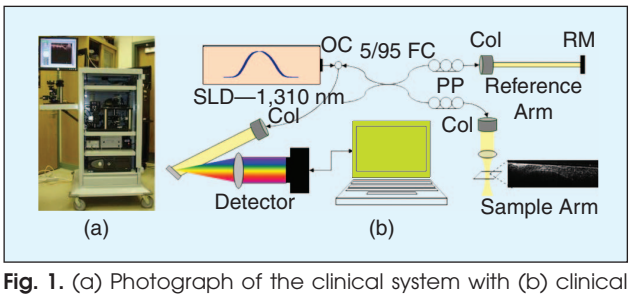

Fig. 1. (a) Photograph of the clinical system with (b) clinical spectral domain optical coherence tomography system schematic. Light from a superluminescent diode (SLD) centered at 1,310 nm is directed into the optical circulator (OC) that passes the light into the fiber coupler (FC) that splits the light into the reference arm (5%) and the sample arm (95%). The light is collimated through a set of fiber collimators (Col). The reflected light from each arm is coupled back together through a set of polarization paddles (PP) and interfered with each other through the 5/95 fiber coupler (FC) and spectrally dispersed onto a line scan camera that serves as the detector.

OCT in Breast Cancer

OCT is a high-resolution microscopic optical imaging technique that yields real-time multidimensional images of subsurface tissue structure [18]–[24]. The use of NIR light enables micron-scale resolution, providing structural images on a resolution scale similar to histopathology. The penetration depth in tissue has been found to be 1–2 mm and is highly dependent on the type of tissue imaged. OCT has been investigated in a large number of clinical applications ranging from ophthalmology, cardiovascular disease, Barrett's esophagus, and more recently in oncology [25]. OCT has also been used to image tumor margins for breast cancer in an NMU carcinogen-induced rat mammary model and intraoperatively for the assessment of tumor margins [21], [26], [27]. High-scattering signals are often attributed to a combination of the increase in nuclear-to-cytoplasm (*N/C*) ratio and the increase in cellular density during the focal proliferation of cancer cells [28], [29]. OCT is a suitable imaging modality for assessing the lymph-node architecture [30] but, more importantly, for imaging and assessing the morphological changes observed in the cortex, which can be used to differentiate between normal nodes and reactive and metastatic nodes. By imaging through the capsule of an intact lymph node, OCT can provide this assessment without compromising the structural integrity of the lymph node, making it a potential candidate as an in vivo nodal-assessment technique.

Materials and Methods

Instrument

A clinical spectral domain OCT (SD-OCT) system [31] was used to assess sentinel lymph nodes for this feasibility imaging study (Figure 1). The OCT system employed a superluminescent diode (B&W Tek Inc., SLD1C), centered at 1,310 nm with a bandwidth of 92 nm. A 60-mm achromatic lens was used to focus 4.75 mW of light to a 35.0-μm spot size (transverse resolution) with an in-focus depth-of-field (confocal parameter) of 1.47 mm. The broad bandwidth of the source resulted in an axial resolution of 8.3 μm in free space or 5.9 μm in tissue. The penetration depth of OCT imaging was 1–2 mm in the axillary lymph nodes. With camera exposure times ranging from 24.4 to 408.4 μs, the measured signal-to-noise ratio (SNR) ranged from 96 to 116 dB, respectively. The imaging system acquired OCT images at a rate of 5,000 axial scans per second or approximately eight frames per second for an image with 600 axial scans covering a lateral distance of 10 mm. A commercial OCT system with similar instrument specifications and performance parameters as the custom-built

Lymph nodes serve as the primary site for filtering, sequestering, and degrading foreign particles that travel through the lymphatic system.

system used for this study was also used. Both systems used light sources centered at 1,310 nm with a bandwidth of 90–100 nm, used the same detection system, and had similar optical elements in the sample arm, yielding comparable axial and transverse resolutions. The main difference between the two systems was in the beam-scanning mechanism, which enabled the custom-built system to scan over longer lateral distances (10 mm) to produce two-dimensional (2-D) images, while the commercial system was able to scan more than a 5×5 mm^2 region to produce three-dimensional (3-D) volumetric images. The acquisition times were approximately 25 s for a single 2-D image (10 mm) for the custom-built system and approximately 25 s for a full 3-D volumetric block of images (5×5 mm^2) for the commercial OCT system.

Imaging Protocol

The patients identified and recruited for this study had primary breast tumors (invasive and/or in situ carcinoma) in need of surgical resection and/or sentinel lymph-node dissection, as determined by their physicians at Carle Foundation Hospital and Carle Clinic Association, Urbana, Illinois, based on previous radiological films, biopsy results, and other relevant diagnostic information. Patients were consented before each surgery based on the approved protocols from the Institutional Review Boards at the University of Illinois at Urbana-Champaign and Carle Foundation Hospital. After resection of the sentinel and/or axillary lymph node(s) by the surgeon and before microscopic assessment by the pathologist, the lymph node was imaged in the operating room using the clinical OCT system. Of the lymph nodes resected during each procedure, one sentinel lymph node, as determined by the surgeon, was imaged per patient for this feasibility study. In cases with multiple sentinel lymph nodes, only the first resected sentinel node was chosen and imaged. No additional nodes were imaged because of time constraints, and no other criteria were used in determining which lymph node would be imaged. In cases where the sentinel lymph node could not be clearly distinguished from other resected lymph nodes, the first axillary lymph node excised was imaged. The intact outer capsule of the sentinel lymph node was exposed for imaging without affecting the structural integrity of the tissue specimen. The OCT beam was laterally scanned across the node over a 10-mm distance to produce a 2-D cross-sectional OCT image. Subsequently, multiple parallel OCT images (spaced 1 mm apart) were acquired orthogonal to the long axis of the node. In cases where the commercial OCT system was used, 5×5 mm^2 regions of images were acquired covering the entire node. Upon completion of the imaging session, the sentinel node was returned to the surgical staff for standard specimen processing and transported to the pathology department for sectioning, staining, and histopathological analysis.

OCT Image Processing and Evaluation Protocol

OCT images were standardized by subtracting the background power spectrum from the raw data, resampling the data using the cubic spline interpolation technique, and displaying the images on the same intensity scale to account for day-to-day system variations. The background power spectrum was acquired by acquiring an image with the sample arm blocked, and recording the power spectrum of the light reflected in the reference arm. This process removes image artifacts that are inherent to the OCT system at the time of imaging. Fifteen patients were enrolled as part of this study to evaluate the potential of OCT imaging for the real-time intraoperative assessment of lymph nodes using the custom-built system. Two patients were enrolled additionally to evaluate the commercial OCT system and the advantages of 3-D volumetric data acquisition. OCT images were evaluated by a single interpreter intraoperatively, allowing for consistent identification of suspicious areas based on the level and distribution of scattering intensity in the outer layers and cortex of the nodes, and the ability to distinguish the boundary between the capsule and cortex of the nodes. Since nodal status is not currently determined intraoperatively by surgeons but rather postoperatively by pathologists, no information about the nodes was transmitted between the surgeons or surgical staff and the researcher imaging and evaluating the OCT images. Using these image features, a single researcher in a single setting evaluated and classified OCT images into normal and abnormal categories where both metastatic and reactive nodes were considered abnormal.

Histopathological Image Evaluation Protocol

According to the standard of care, the sentinel lymph node was bisected, paraffin embedded, and sectioned for histopathological analysis in the pathology department. The tissue sections were stained with hematoxylin and eosin (H&E) and in some cases also stained immunohistochemically for CK7 to further confirm the presence of and to characterize the cancer cells in the sentinel node. The histology slides were digitized using a light microscope at 4× magnification and autostitched together (Adobe Photoshop CS3) to provide a single montage for viewing and comparison purposes. The H&E-stained histology slides were reviewed by board-certified pathologists and classified as normal, reactive, or metastatic. The histopathological processing and analysis were performed as part of the standard of care and reported by the pathology department.

Results

Specimen Information

A total of 30 sentinel lymph nodes and an additional 106 axillary lymph nodes were surgically resected from 17 patients as

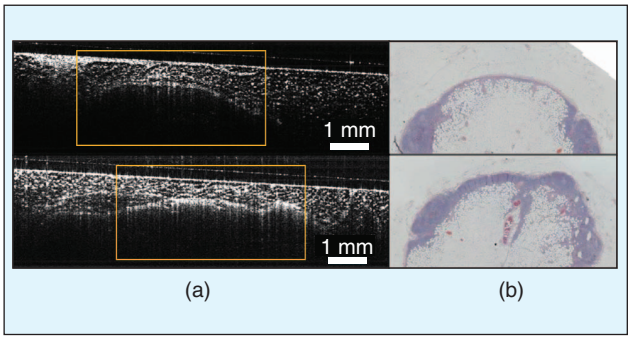

Fig. 2. (a) Normal lymph node – OCT images from a normal sentinel lymph node with (b) corresponding H&E histology demonstrate an intact capsule structure, which is easily distinguishable from the cortex of the lymph node. The OCT images are highlighted (orange boxes) with the regions that correlate with the histology images.

determined by the surgeons as part of the standard of care. A subset (16 sentinel, one axillary) of the lymph nodes (one per patient) chosen, based on the order they were resected, were imaged with OCT intraoperatively. Of all the nodes resected, 11 (8%) were found to be metastatic and even fewer, 2 (1%) were found to be reactive, resulting in 91% of all nodes resected being classified as normal. When considering only the sentinel lymph nodes as labeled by the surgeons, four of the 30 (13%) sentinel lymph nodes and one of the 30 (3%) were classified as metastatic and reactive, respectively, by histopathological analysis, resulting in 84% of the sentinel nodes being reported as normal. OCT images of 17 lymph nodes from 17 patients were used to identify unique image features that could potentially be used to classify lymph nodes as normal, reactive, or metastatic. OCT images were acquired from 16 of the 30 sentinel lymph nodes from 16 patients, and one axillary lymph node from the 17th patient, where identification of the sentinel node was not possible by the surgeon. Of the 17 nodes imaged with OCT, histopathological analysis classified three nodes as metastatic, one node as reactive, and the remaining 13 nodes as normal. The OCT images from two of the three metastatic nodes were excluded from the study, as they could not be adequately interpreted as the node capsule was not well exposed from the surrounding fatty tissue, placing the nodal architectural features beyond the imaging depth of OCT. The third metastatic node was imaged using the commercial OCT system.

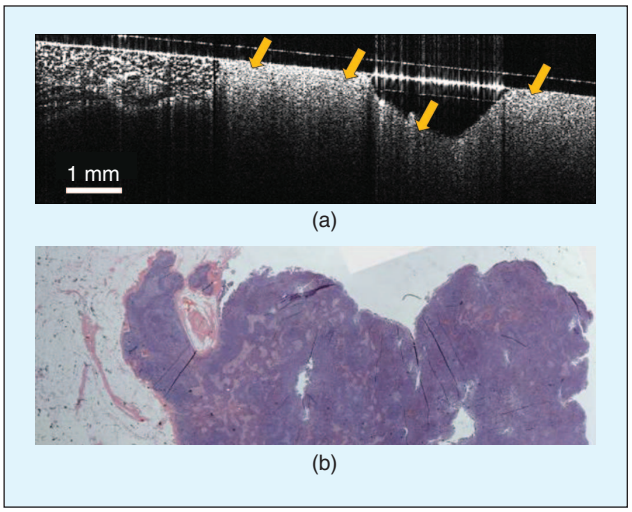

Fig. 3. (a) Reactive lymph node – OCT image from a reactive axillary lymph node with (b) corresponding H&E histology. In this case, the increased cellular density in the cortex when the lymph node becomes reactive contributes to the increased scattering signal observed under OCT. The change in scattering intensity begins to match the scattering intensity of the capsule, decreasing the ability to distinguish the capsule from the cortex under the OCT images (arrows).

Representative OCT Images

Representative intraoperative images from normal (Figures 2 and 4), reactive (Figure 3), and metastatic (Figure 5) axillary lymph nodes are shown. The normal lymph nodes are all characterized by a distinct capsule that is highly scattering, in comparison to the lower scattering cortex, as seen in the representative OCT images (Figures 2 and 4). Under OCT, the transverse sinuses separating the lymphoid follicles of the lymph node can be observed in Figure 4. The corresponding H&E-stained histological slides show normal nodes with expected architecture that are either largely lipid filled (Figure 2) or contain more eosinophilic (pink) structures indicative of the presence of intracellular and extracellular proteins (Figure 4). The subcapsular sinus separates the capsule from the cortex, which is organized into discrete lymphoid nodules with germinal centers observable in normal lymph nodes. The distinct boundary between the capsule and the cortex is no longer visible in reactive (Figure 3) and metastatic (Figure 5) nodes where the entire node becomes more highly scattering, matching the scattering intensity level from the capsule, and forming a single homogeneous scattering layer.

The corresponding H&E histology slides presented in Figures 3 and 5 have more basophilic structures as exhibited by the darker blue stain, which stains for the nucleic acids found in the ribosomes, the chromatins in the nucleus, and the RNA in the cytoplasm. The metastatic lymph node shows a loss of

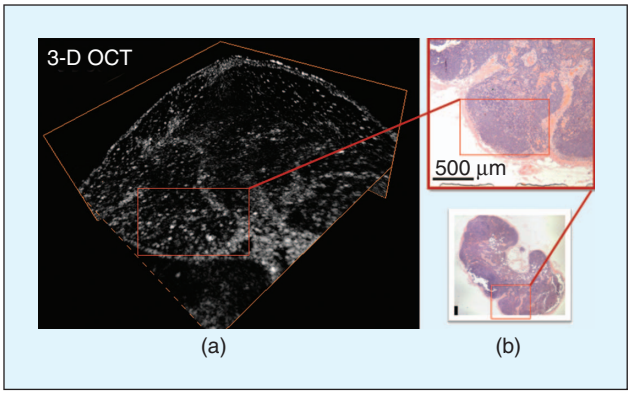

Fig. 4. Three-dimensional rendering of a normal lymph node. (a) OCT image volume acquired from a normal sentinel lymph node is shown with (b) the corresponding H&E histology. The normal lymph node shows a clear capsule that is easily differentiated from the low-scattering cortex. The OCT images correlate to the regions in the histology that are highlighted by the red boxes. The OCT image block measures $5 \times 5 \times 1.7$ mm^3.

Optical coherence tomography is a high-resolution microscopic optical imaging technique that yields real-time multidimensional images of subsurface tissue structure.

normal tissue architecture as there is an obvious lymphoid depletion characterized by a decrease in the number and size of follicles with some or no germinal centers. At the same time, the decrease of sinus spaces and increased density of cells observed is due to the high level of cancer-cell proliferation.

Three-dimensional OCT reconstructions are presented in Figures 4 and 5, demonstrating the added level of details available through the reconstructions. These renderings identify the same features as those found in the 2-D images but further allows for the arbitrary optical sectioning of the tissue along planes that are not necessarily the same as the OCT imaging acquisition planes. These intraoperative findings from human lymph nodes extend our observations from previously reported OCT image data of lymph nodes from a rat mammary model [30]. The normal rat lymph node exhibited a highly scattering layer corresponding to the capsule, compared with the low-scattering cortex [30]. In the same report, OCT images from a necrotic metastatic lymph node exhibited a high level of scattering intensity and capsule disruption.

Discussion

The relatively high percentage of normal nodes resected during lymph-node dissection procedures, as was exhibited for the patients enrolled in this study, points to the significant need for a real-time intraoperative microscopic nodal-assessment technology. OCT has the potential to fill this crucial role by providing real-time intraoperative information through the identification of unique architectural features observed in the capsule and outer cortex of the lymph node. These features correspond to known morphological changes in reactive and metastatic lymph nodes and are all accessible within the penetration depth of OCT.

Identification of Normal Nodes from Reactive and Metastatic Lymph Nodes

When cancer cells metastasize through the lymphatic system, the nodes serve as the primary line of defense to sequester the cancer cells and initiate a tumor-specific immunological response. This process will initially cause an enlargement of the lymph node as a part of the reactive inflammatory response, but this enlargement can also be attributed to the replication of cancer cells in the nodes. The presence of inflammation in the node, however, is not sufficient to indicate the presence of cancer cells. With hypercellularity, either from the inflammatory response or from the replication and expansion of cancer cells, the lymph node will not only increase in relative size but also increase in cellular density within the node. These changes will typically correspond to an increase in the scattering observed in OCT, matching the scattering levels observed in the capsule. As the scattering intensity in the capsule and cortex areas become similar, the differentiation of the capsule from the cortex becomes less distinct. The increased scattering changes observed in the cortex of reactive and metastatic nodes are more likely due to increased cellular density but could also be attributed to the increased number of cancer cells that have a higher N/C ratio. These changes are more predominant in the cortex region where the germinal centers and follicles, the primary sites of lymphocyte recruitment and aggregation, are located.

Potential Clinical Impact

It is recognized that the majority of lymph nodes resected for staging purposes are negative, and that the clinically relevant data from lymph node resection is primarily to know whether or not the lymph node contains metastatic disease. In addition, the primary surgical risk factor for lymphedema is nodal dissection of the axillary lymph nodes, as well as the associated scarring from surgical intervention. Therefore, reducing the number or eliminating the need to resect normal nodes during surgery will not only reduce the number of lymph nodes resected but also decrease the risk of developing lymphedema. With a 1–2-mm imaging penetration depth, OCT is a suitable modality to visualize the microscopic lymph-node architecture, including the

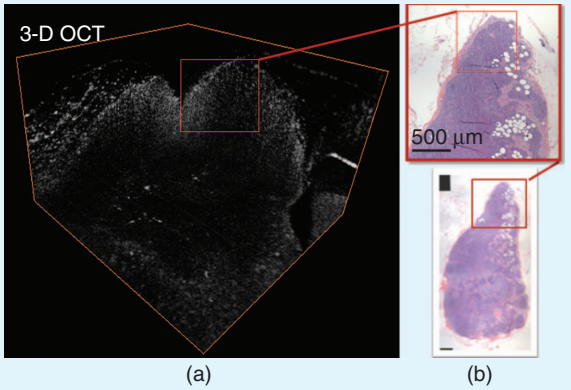

Fig. 5. Three-dimensional rendering of a metastatic lymph node. (a) OCT image volume acquired from a metastatic axillary lymph node in a single session is shown with (b) the corresponding H&E histology. As with reactive lymph nodes, increased scattering from the node is observed in the OCT data, and the ability to differentiate distinct boundaries between the node capsule and cortex has been lost. The OCT images correlate to the regions in the histology that are highlighted by the red boxes. The OCT image block measures $5 \times 5 \times 1.7$ mm^3.

The primary surgical risk factor for lymphedema is dissection of lymph nodes, as well as the associated scarring from surgical intervention.

capsule and the outer cortex containing the follicles and germinal centers. In normal nodes, OCT is capable of clearly defining the boundary between the capsule and the cortex based on the scattering intensities. This boundary is lost in abnormal lymph nodes. With no suitable real-time intraoperative method to assess the lymph node before its surgical resection, OCT is able to fill a niche by providing high-resolution microscopic images in real time. Histopathological analysis from paraffin sections, the current standard of care, is unable to provide surgeons with this real-time information on the nodal status that could be used to guide the surgical resection of lymph nodes. OCT is capable of providing this information intraoperatively in real time, with the potential for in vivo or in situ imaging, thereby potentially eliminating the need for further lymph-node resections and reducing the number of resulting complications.

Future Directions

The intraoperative OCT imaging data from the lymph nodes in this feasibility study demonstrate promising results. From the images presented, distinct morphological differences are observed between the defined classifications of lymph nodes, which are all well correlated to the corresponding histopathological findings and are all within the penetration depth of the OCT imaging system. These initial intraoperative ex vivo imaging studies demonstrate that the relevant diagnostic information needed to classify lymph nodes is accessible by OCT from outside of the lymph node capsule, leaving the lymph node structurally intact. Transcapsule imaging by OCT, along with the implementation of a fast scanning handheld probe [32], will allow lymph nodes to be rapidly imaged in situ. Needle-based OCT imaging probes would allow further minimally invasive probing of the node if it is not fully exposed or easily accessible, such as in performing transcutaneous needle-biopsy procedures of lymph nodes [33]–[35].

Future in vivo studies will further determine the clinical impact of OCT on reducing the number of normal lymph nodes removed and subsequently reducing the rate of morbid complications associated with lymph node dissections and breast cancer surgeries. The implementation of recent technological advances to further increase the resolution of OCT [36] and data acquisition speed [37] and to computationally classify tissue types [27], [33] will improve the usability and effectiveness of OCT in the intraoperative assessment of lymph nodes by enhancing the capability to examine the underlying lymph node microarchitecture, by rendering 3-D OCT data sets for multisectional assessment and by rapidly classifying features and tissue types using computer-aided detection.

Acknowledgments

This study was supported by the National Institutes of Health NIBIB, R01 EB005221, Carle Foundational Hospital, and the Grainger Foundation. Stephen A. Boppart is the principal investigator on all of these grants and he also receives patent royalties from the Massachusetts Institute of Technology for technologies associated with OCT. Freddy T. Nguyen was supported by the U.S. Department of Defense grant BC073292. The authors acknowledge the technical contributions of Dr. Daniel Marks, the assistance with histological analysis by Dr. Marina Marjanovic, and the contributions of Ann Benefiel, Mary Collins, and Barbara Hall in the recruitment and consenting of patients. They also thank the physicians, staff, and administration at Carle Foundation Hospital and Carle Clinic Association for their assistance in this research. Additional information can be found at http://biophotonics.illinois.edu.

Freddy T. Nguyen received the B.S. degree in chemistry and the B.A. degree in mathematics from Rice University in 2002. Since 2003, he has been at the University of Illinois at Urbana-Champaign where he is an M.D.–Ph.D. candidate. He currently holds a predoctoral fellowship from the Department of Defense's Congressionally Directed Medical Research Programs—Breast Cancer Program. He was a research engineer in the G.R. Harrison Spectroscopy Laboratory at the Massachusetts Institute of Technology from 2002 to 2003. He is a member of the American Medical Association, the American Association for the Advancement of Science, the American Association for Cancer Research, and the American Chemical Society. His research interests have broadly been in the development of spectroscopic and imaging techniques and their associated contrast agents for direct biomedical applications such as cancer and atherosclerosis.

Adam M. Zysk received the B.S., M.S., and Ph.D. degrees in electrical engineering from Purdue University and the University of Illinois at Urbana-Champaign in 2001, 2003, and 2007, respectively. Since 2007, he has been a postdoctoral researcher in the Electrical and Computer Engineering Department, Illinois Institute of Technology, Chicago, Illinois. As a graduate student, his research focused on the application of OCT to breast-cancer imaging. He currently researches phase-contrast X-ray imaging techniques and their medical applications. He is a Member of the IEEE, a member of the Optical Society of America, a member in training of the Radiological Society of North America, and a member of the SPIE.

Eric J. Chaney received the B.S. degree in biology from the University of Evansville, Evansville, Indiana, in 1992. From

1993 to 1997, he worked as a research assistant at the Indiana University School of Medicine, Indiana State University, Terre Haute. From 1997 to 2000, he worked as a transmission electron microscope technician at the University of Illinois, Urbana-Champaign, Urbana. Since 2000, he has been a research specialist in molecular biology at the Biophotonics Imaging Laboratory, Beckman Institute, University of Illinois, Urbana-Champaign.

Steven G. Adie received a B.Sc. (Hons.) degree in chemical physics in 1997 and a Ph.D. degree in electrical and electronic engineering in 2007, both from the University of Western Australia. Between his undergraduate and graduate studies, he worked as a research engineer at a company developing new technologies for LASIK eye surgery. He has been a postdoctoral research associate in the Biophotonics Imaging Laboratory at the Beckman Institute, University of Illinois at Urbana-Champaign since 2007. His research interests include development of low-coherence imaging techniques, namely interferometric synthetic aperture microscopy and OCT, and their application to breast cancer imaging. His Ph.D. research was on the development of alternate contrast mechanisms for OCT.

Jan G. Kotynek received a B.A. degree in psychology in 1971 followed by an M.D. degree in 1975 from the University of Illinois. He then completed a residency in surgery at the University of Wisconsin in 1982. Since then, he has practiced as a general surgeon, the last 18 years at Carle Clinic, and has served on the faculty of the University of Illinois as clinical assistant professor of surgery. In 2008, he retired from clinical practice. He is a member of the American College of Surgeons, Illinois Surgical Society, American Medical Association, and Alpha Omega Alpha Honor Medical Society.

Uretz J. Oliphant received the B.A. degree from Boston University and the M.D. degree from the University of Minnesota in 1983. He completed an internship in general surgery at the University of Chicago in 1985, residency in general surgery at the University of Illinois in 1991, and a fellowship in trauma/critical care at the Illinois Masonic Medical Center. Since 1992, he has been a surgeon at the Carle Clinic. Since 1994, he has been a professor in clinical surgery and internal medicine at the University of Illinois, Urbana-Champaign. He is currently the head of the Department of Surgery at the University of Illinois College of Medicine, Urbana-Champaign. He is a member of the American Medical Association, the American Society of Breast Surgeons, president of the Illinois Surgical Society, and a fellow of the International College of Surgeons.

Frank J. Bellafiore received the B.S. degree in mathematics and chemistry from Creighton University, Omaha, Nebraska, in 1986, and the M.D. degree from Washington University,

St. Louis, in 1990. He completed a residency in anatomic and clinical pathology, including a fellowship in surgical pathology and cytopathology in 1995 at the University of Virginia Health Sciences Center. He is currently a pathologist and director of histology and flow cytometry in the Department of Pathology at the Carle Clinic Association. He is a clinical assistant professor at the University of Illinois College of Medicine, Urbana-Champaign.

Kendrith M. Rowland received the B.A. degree from Lawrence University, Appleton, Wisconsin, in 1976, and the M.D. degree from the University of Illinois College of Medicine, Chicago, in 1980. He completed a residency in internal medicine at the University of Illinois Hospital, Westside V.A., and a fellowship in oncology at Rush-Presbyterian, St. Luke's Medical Center. He is currently a hematologist and oncologist in the Department of Medicine at the Carle Clinic Association and Carle Foundation Hospital since 1985. He is the principal investigator of the Carle Cancer Center—Community Clinical Oncology Program. He is a clinical assistant professor of medicine at the University of Illinois College of Medicine, Urbana-Champaign. He is a member of the American Society of Clinical Oncology, the International Association of the Study of Lung Cancer, Phi Beta Kappa, and the ASCO Clinical Trials Committee.

Patricia A. Johnson earned a B.S. degree in microbiology from the University of Maryland in 1969, and M.S. and Ph.D. degrees in microbiology from the University of Illinois in 1970 and 1974, respectively, and M.D. degree at Rush University Medical School in 1977. She completed a residency in internal medicine in 1980 and a fellowship in medical oncology in 1982 at Rush Presbyterian St. Luke's Medical Center, Chicago. She has been a medical oncologist at Carle Clinic, Urbana Illinois since 1982, where she has served as president of the medical staff, chair of the board of governors, medical director of medical subspecialties, and medical director of the Mills Breast Cancer Institute. She is a member of American Society of Clinical Oncology, American Medical Association, Illinois State Medical Society, Champaign County Medical Society, Phi Beta Kappa, Phi Sigma, Phi Kappa Phi, Sigma Alpha Omicron, and Alpha Lambda Delta.

Stephen A. Boppart received the B.S. degree in electrical and bioengineering and the M.S. degree in electrical engineering from the University of Illinois, Urbana-Champaign, in 1990 and 1991, respectively, the Ph.D. degree in electrical and medical engineering from the Massachusetts Institute of Technology, in 1998, and the M.D. degree from Harvard Medical School, in 2000. He completed residency training in internal medicine at the University of Illinois, Urbana-Champaign, in 2005. He is currently a professor of electrical and computer engineering,

bioengineering, and medicine. His research interests include the development and translation of novel optical-imaging technologies for biological and medical applications, with particular emphasis in cancer detection and diagnosis. He is a Senior Member of the IEEE. He is a fellow of the Optical Society of America and the International Society for Optical Engineering (SPIE). In 2003, he was named as one of the Top 100 Young Innovators in the world by MIT's *Technology Review Magazine* for advances in medical imaging technology. He received the IEEE Engineering in Medicine and Biology Society Early Career Achievement Award in 2005.

Address for Correspondence: Stephen A. Boppart, Beckman Institute for Advanced Science and Technology, University of Illinois at Urbana-Champaign, 405 North Mathews Avenue, Urbana , IL 61801, USA. E-mail: boppart@illinois.edu.

References

[1] *Cancer Facts & Figures 2009*, Atlanta: American Cancer Society, 2009.
[2] *Breast Cancer Facts & Figures 2007–2008*, Atlanta: American Cancer Society, 2008.
[3] D. Krag, D. Weaver, T. Ashikaga, F. Moffat, V. S. Klimberg, C. Shriver, S. Feldman, R. Kusminsky, M. Gadd, J. Kuhn, S. Harlow, and P. Beitsch, "The sentinel node in breast cancer–a multicenter validation study," *N. Engl. J. Med.*, vol. 339, pp. 941–946, Oct. 1998.
[4] J. V. Frangioni, S. W. Kim, S. Ohnishi, S. Kim, and M. G. Bawendi, "Sentinel lymph node mapping with Type-II quantum dots," *Methods Mol. Biol.*, vol. 374, pp. 147–160, 2007.
[5] S. Kim, Y. T. Lim, E. G. Soltesz, A. M. De Grand, J. Lee, A. Nakayama, J. A. Parker, T. Mihaljevic, R. G. Laurence, D. M. Dor, L. H. Cohn, M. G. Bawendi, and J. V. Frangioni, "Near-infrared fluorescent type II quantum dots for sentinel lymph node mapping," *Nat. Biotechnol.*, vol. 22, pp. 93–97, Jan. 2004.
[6] H. Nimura, N. Narimiya, N. Mitsumori, Y. Yamazaki, K. Yanaga, and M. Urashima, "Infrared ray electronic endoscopy combined with indocyanine green injection for detection of sentinel nodes of patients with gastric cancer," *Br. J. Surg.*, vol. 91, pp. 575–579, May 2004.
[7] S. A. Mclaughlin, L. M. Ochoa-Frongia, S. M. Patil, H. S. Cody III, and L. M. Sclafani, "Influence of frozen-section analysis of sentinel lymph node and lumpectomy margin status on reoperation rates in patients undergoing breast-conservation therapy," *J. Am. Coll. Surg.*, vol. 206, pp. 76–82, Jan. 2008.
[8] R. Ali, A. M. Hanly, P. Naughton, C. F. Castineira, R. Landers, R. A. Cahill, and R. G. Watson, "Intraoperative frozen section assessment of sentinel lymph nodes in the operative management of women with symptomatic breast cancer," *World J. Surg. Oncol.*, vol. 6, p. 69, 2008.
[9] K. Motomura, S. Nagumo, Y. Komoike, H. Koyama, and H. Inaji, "Accuracy of imprint cytology for intraoperative diagnosis of sentinel node metastases in breast cancer," *Ann. Surg.*, vol. 247, pp. 839–842, May 2008.
[10] A. J. Creager, K. R. Geisinger, S. A. Shiver, N. D. Perrier, P. Shen, J. Ann Shaw, P. R. Young, and E. A. Levine, "Intraoperative evaluation of sentinel lymph nodes for metastatic breast carcinoma by imprint cytology," *Mod. Pathol.*, vol. 15, pp. 1140–1147, Nov. 2002.
[11] T. B. Julian, P. Blumencranz, K. Deck, P. Whitworth, D. A. Berry, S. M. Berry, A. Rosenberg, A. B. Chagpar, D. Reintgen, P. Beitsch, R. Simmons, S. Saha, E. P. Mamounas, and A. Giuliano, "Novel intraoperative molecular test for sentinel lymph node metastases in patients with early-stage breast cancer," *J. Clin. Oncol.*, vol. 26, pp. 3338–3345, July 2008.
[12] B. Bird, M. Miljkovic, M. J. Romeo, J. Smith, N. Stone, M. W. George, and M. Diem, "Infrared micro-spectral imaging: Distinction of tissue types in axillary lymph node histology," *BMC Clin. Pathol.*, vol. 8, p. 8, 2008.
[13] E. M. Sevick-Muraca, R. Sharma, J. C. Rasmussen, M. V. Marshall, J. A. Wendt, H. Q. Pham, E. Bonefas, J. P. Houston, L. Sampath, K. E. Adams, D. K. Blanchard, R. E. Fisher, S. B. Chiang, R. Elledge, and M. E. Mawad, "Imaging of lymph flow in breast cancer patients after microdose administration of a near-infrared fluorophore: Feasibility study," *Radiology*, vol. 246, pp. 734–741, Mar. 2008.
[14] R. Sharma, J. A. Wendt, J. C. Rasmussen, K. E. Adams, M. V. Marshall, and E. M. Sevick-Muraca, "New horizons for imaging lymphatic function," *Ann. N. Y. Acad. Sci.*, vol. 1131, pp. 13–36, 2008.
[15] H. L. Bumpers, I. M. Best, D. Norman, and W. L. Weaver, "Debilitating lymphedema of the upper extremity after treatment of breast cancer," *Amer. J. Clin. Oncol.*, vol. 25, pp. 365–367, Aug. 2002.
[16] I. Langer, U. Guller, G. Berclaz, O. R. Koechli, G. Schaer, M. K. Fehr, T. Hess, D. Oertli, L. Bronz, B. Schnarwyler, E. Wight, U. Uehlinger, E. Infanger, D. Burger, and M. Zuber, "Morbidity of sentinel lymph node biopsy (SLN) alone versus SLN and completion axillary lymph node dissection after breast cancer surgery: a prospective Swiss multicenter study on 659 patients," *Ann. Surg.*, vol. 245, pp. 452–461, Mar. 2007.
[17] M. de Boer, C. H. van Deurzen, J. A. van Dijck, G. F. Borm, P. J. van Diest, E. M. Adang, J. W. Nortier, E. J. Rutgers, C. Seynaeve, M. B. Menke-Pluymers, P. Bult, and V. C. Tjan-Heijnen, "Micrometastases or isolated tumor cells and the outcome of breast cancer," *N. Engl. J. Med.*, vol. 361, pp. 653–663, Aug. 2009.
[18] S. A. Boppart, B. E. Bouma, C. Pitris, J. F. Southern, M. E. Brezinski, and J. G. Fujimoto, "In vivo cellular optical coherence tomography imaging," *Nat. Med.*, vol. 4, pp. 861–865, July 1998.
[19] S. A. Boppart, B. E. Bouma, C. Pitris, G. J. Tearney, J. F. Southern, M. E. Brezinski, and J. G. Fujimoto, "Intraoperative assessment of microsurgery with three-dimensional optical coherence tomography," *Radiology*, vol. 208, pp. 81–86, July 1998.
[20] S. A. Boppart, T. F. Deutsch, and D. W. Rattner, "Optical imaging technology in minimally invasive surgery. Current status and future directions," *Surg. Endosc.*, vol. 13, pp. 718–722, July 1999.
[21] S. A. Boppart, W. Luo , D. L. Marks, and K. W. Singletary, "Optical coherence tomography: Feasibility for basic research and image-guided surgery of breast cancer," *Breast Cancer. Res. Treat.*, vol. 84, pp. 85–97, Mar. 2004.
[22] B. E. Bouma and G. J. Tearney, *Handbook of Optical Coherence Tomography*. New York: Marcel Dekker, 2002.
[23] J. G. Fujimoto, C. Pitris, S. A. Boppart, and M. E. Brezinski, "Optical coherence tomography: An emerging technology for biomedical imaging and optical biopsy," *Neoplasia*, vol. 2, pp. 9–25, Jan.–Apr. 2000.
[24] D. Huang, E. A. Swanson, C. P. Lin, J. S. Schuman, W. G. Stinson, W. Chang, M. R. Hee, T. Flotte, K. Gregory, C. A. Puliafito, and J. G. Fujimoto, "Optical coherence tomography," *Science*, vol. 254, pp. 1178–1181, Nov. 1991.
[25] A. M. Zysk, F. T. Nguyen, A. L. Oldenburg, D. L. Marks, and S. A. Boppart, "Optical coherence tomography: A review of clinical development from bench to bedside," *J. Biomed. Opt.*, vol. 12, p. 051403, Sept.–Oct. 2007.
[26] F. Nguyen, A. M. Zysk, E. J Chaney, J. G. Kotynek, U. Oliphant, F. J. Bellafiore, K. M. Rowland, P. A. Johnson, and S. A. Boppart, "Intraoperative evaluation of breast tumor margins with optical coherence tomography," *Cancer. Res* , vol. 69, pp. 8790–8796, Nov. 2009.
[27] A. M. Zysk and S. A. Boppart, "Computational methods for analysis of human breast tumor tissue in optical coherence tomography images," *J. Biomed. Opt.*, vol. 11, p. 054015, Sept.–Oct. 2006.
[28] D. Arifler, et al., "Light scattering from normal and dysplastic cervical cells at different epithelial depths: Finite-difference time-domain modeling with a perfectly matched layer boundary condition," *J. Biomed. Opt.*, vol. 8, pp. 484–494, July 2003.
[29] R. Drezek, et al., "Light scattering from cervical cells throughout neoplastic progression: Influence of nuclear morphology, DNA content, and chromatin texture," *J. Biomed. Opt.*, vol. 8, pp. 7–16, Jan. 2003.
[30] W. Luo, et al., "Optical biopsy of lymph node morphology using optical coherence tomography," *Technol. Cancer. Res. Treat.*, vol. 4, pp. 539–548, Oct. 2005.
[31] F. T. Nguyen, A. M. Zysk, J. G. Kotynek, F. J. Bellafiore, K. M. Rowland, P. A. Johnson, E. J. Chaney, and S. A. Boppart, "Portable real-time optical coherence tomography system for intraoperative imaging and staging of breast cancer," in *Proc. SPIE—Photonics West BiOS—Advanced Biomedical and Clinical Diagnostic Systems V*, San Jose, CA, 2007.
[32] X. Liu, M. J. Cobb, Y. Chen, M. B. Kimmey, and X. Li, "Rapid-scanning forward-imaging miniature endoscope for real-time optical coherence tomography," *Opt. Lett.*, vol. 29, pp. 1763–1765, Aug. 2004.
[33] B. D. Goldberg, N. V. Iftimia, J. E. Bressner, M. B. Pitman, E. Halpern, B. E. Bouma, and G. J. Tearney, "Automated algorithm for differentiation of human breast tissue using low coherence interferometry for fine needle aspiration biopsy guidance," *J. Biomed. Opt.*, vol. 13, p. 014014, Jan.–Feb. 2008.
[34] A. M. Zysk, S. G. Adie, J. J. Armstrong, M. S. Leigh, A. Paduch, D. D. Sampson, F. T. Nguyen, and S. A. Boppart, "Needle-based refractive index measurement using low-coherence interferometry," *Opt. Lett.*, vol. 32, pp. 385–387, Feb. 2007.
[35] A. M. Zysk, E. J. Chaney, and S. A. Boppart, "Refractive index of carcinogen-induced rat mammary tumours," *Phys. Med. Biol.*, vol. 51, pp. 2165–2177, May 2006.
[36] R. J. Zawadzki, B. Cense, Y. Zhang, S. S. Choi, D. T. Miller, and J. S. Werner, "Ultrahigh-resolution optical coherence tomography with monochromatic and chromatic aberration correction," *Opt. Express.*, vol. 16, pp. 8126–8143, May 2008.
[37] R. Huber, D. C. Adler, and J. G. Fujimoto, "Buffered Fourier domain mode locking: Unidirectional swept laser sources for optical coherence tomography imaging at 370,000 lines/s," *Opt. Lett.*, vol. 31, pp. 2975–2977, Oct. 2006.